

1 **South-western Africa vegetation responses to atmospheric and oceanic**
2 **changes during the last climatic cycle**

3
4 D.H. Urrego^{1,2*}, M.F. Sánchez Goñi¹, A.-L. Daniau³, S. Lechevrel⁴, V. Hanquiez⁴
5

6 ¹Ecole Pratique des Hautes Etudes EPHE, Université de Bordeaux, Environnements et

7 Paléoenvironnements Océaniques et Continentaux (EPOC), Unité Mixte de Recherche 5805, F-
8 33615 Pessac, France.

9 ²Geography, College of Life and Environmental Sciences, University of Exeter, United Kingdom.

10 ³Centre National de la Recherche Scientifique CNRS, Université de Bordeaux, Environnements et

11 Paléoenvironnements Océaniques et Continentaux (EPOC), Unité Mixte de Recherche 5805, F-
12 33615 Pessac, France.

13 ⁴Université de Bordeaux, Environnements et Paléoenvironnements Océaniques et Continentaux
14 (EPOC), Unité Mixte de Recherche 5805, F-33615 Pessac, France.

15
16 *Corresponding author full address: Geography, College of Life & Environmental Sciences, University
17 of Exeter, Amory Building B302, Rennes Drive, EX4 4RJ, Exeter, United Kingdom. E-mail:
18 d.urrego@exeter.ac.uk. Tel: +44 (0)1392 725874, Fax: +44 (0)1392 723342.
19

20
49 BWS
57 SST
58 ITCZ
93 ka
177 En-LSav
178 Bd-LSav
203 BETH
203 NMDJ
215 MIE
216 AMS^{14c}

107 Fig. 1
125 Fig. 2
182 Suppl Table 1
185 Suppl. Mat.
226 Suppl Fig. 1
234 Suppl Fig. 2
273 Suppl Fig. 3/?
273 Suppl Fig. 5
286 Fig. 3
308 Fig. 4
344 Fig. 5

20

21

22 **Abstract**

23 Terrestrial and marine climatic tracers from marine core MD96-2098 collected in the
24 southwestern African margin and spanning from 194 to 24^{ka} (thousand years before present)
25 documented three pronounced expansions of Nama-Karoo and fine-leaved savanna during the last
26 interglacial (Marine Isotopic Stage 5 – MIS 5). Nama-Karoo and fine-leaved savanna expansions were
27 linked to increased aridity during the three warmest substadials of MIS 5. Enhanced aridity
28 potentially resulted from a combination of reduced ^{explain acronym} BUS, expanded subtropical high-pressure cells,
29 and reduced austral-summer precipitation due to a northward shift of the Intertropical Convergence
30 Zone (ITCZ). Decreased austral-winter precipitation was likely linked to a southern displacement of
31 the westerlies. In contrast, during glacial isotopic stages MIS 6, 4 and 3, Fynbos expanded at the
32 expense of Nama-Karoo and fine-leaved savanna indicating a relative increase in precipitation
33 probably concentrated during the austral winter months. Our record also suggested that warm-cold
34 or cold-warm transitions between isotopic stages and substages were punctuated by short increases
35 in humidity. Increased aridity during MIS 5e, 5c and 5a warm substages coincided with minima in
36 both precessional index and global ice volume. On the other hand, austral-winter precipitation
37 increases were associated with precession maxima at the time of well-developed northern-
38 hemisphere ice caps.

40 **Key words**

41 Benguela upwelling, fine-leaved savanna, Intertropical Convergence Zone (ITCZ), last interglacial,
42 Nama-Karoo, southern westerlies, southwestern Africa.

43

44 **1. Introduction**

Acronyms BUS and ITCZ do not repeat
in the Abstract and, therefore, may be
omitted. Introduce these acronyms
in the Introduction

Introduce acronym here

45 Southern Africa is influenced at present by tropical and subtropical atmospheric circulation
46 linked to ITCZ shifts, and by both the Indian and the Atlantic Oceans (Tyson and Preston-Whyte,
47 2000). The water exchange between the two oceans is termed the Agulhas leakage and is suggested
48 as a potential trigger of meridional overturning circulation changes (Beal et al., 2011; Biastoch et al.,
49 2008). (BUS) also affects climate in southwestern Africa and its strength is linked to arid conditions
50 and to the extent of the coastal Namib Desert (Cowling et al., 1997b). The combination of globally-
51 important atmospheric and oceanic systems linked to the climate of southern Africa make
52 understanding past climate change in the region particularly significant.

53 Whether southern Africa was characterised by aridity or by increased humidity during the
54 last interglacial remains unclear. Previous work using marine markers has documented an
55 intensification of the Agulhas leakage during interglacials (Peeters et al., 2004), which suggests a
56 reduced influence of the subtropical front and reduced precipitation. Other works have shown
57 increased sea surface temperatures (SST) in the Benguela Current during interglacials linked to
58 weakening of BUS (Kirst et al., 1999) and decreased influence of the ^{*in full*} (ITCZ) in southern Africa (Tyson,
59 1999) suggesting its northward migration. These three climatic factors combined would result in a
60 slight increase in humidity in northeastern South Africa during interglacials. On the other hand,
61 increased aridity during the last interglacial in southern Africa has been suggested based on ratios
62 of aeolian dust and fluvial mud in marine sediments (Stuut and Lamy, 2004).

63 Vegetation-based climate reconstructions for southern Africa have been less straight
64 forward given the paucity of records (Dupont, 2011) and fragmentary nature of some terrestrial
65 sequences (Scott et al., 2012; Meadows et al., 2010). On one hand, some records point to expansions
66 of the Fynbos biome (Shi et al., 2001) and the winter-rainfall zone during glacial periods (Chase and
67 Meadows, 2007), and to a contracting Namibian Desert during interglacials (Shi et al., 2000) and the
68 late Holocene (Scott et al., 2012). On the other hand, it has been suggested that savannas expanded
69 southwards during the Holocene climate optimum (Dupont, 2011), and that the southern Africa
70 summer-rainfall zone expanded during interglacials due to a strengthening of the walker circulation

71 and a southward migration of the ITCZ (Tyson, 1999). Contrastingly, significant reductions of austral-
72 summer precipitation in southern Africa are suggested to coincide with precession minima both
73 during glacials and interglacials (Partridge et al., 1997), and are independently supported by
74 reductions of grass-fuelled fires in the subcontinent (Daniau et al., 2013). The latter observations
75 suggest aridity increase and savanna biome reductions, instead of expansions, during the last
76 interglacial precession minima. Whether the last interglacial was characterised by orbitally-driven
77 increased aridity or increased precipitation may have significant implications for resource availability
78 and climate in the region today, hence the importance of further investigating the glacial-interglacial
79 climate dynamics of southern Africa.

80 In this study we aim to disentangle the contrasting hypotheses of orbital-scale climate
81 change in southern Africa by combining terrestrial and marine tracers from the marine sequence
82 MD96-2098. We used pollen and charcoal as terrestrial tracers, and $\delta^{18}\text{O}$ from benthic foraminifera
83 as a marine tracer. Vegetation reconstructions from marine records have contributed to our
84 understanding of ocean-land interactions in many regions of the world, including the Iberian
85 Peninsula (Sánchez Goñi et al., 2000), the eastern subtropical Pacific (Lyle et al., 2012), and the
86 tropical Atlantic (González and Dupont, 2009). Studies from the African margin (e.g. Dupont
87 (2011); Dupont et al. (2000); Dupont and Behling (2006); Hooghiemstra et al. (1992); Leroy and Dupont
88 (1994)) have demonstrated that pollen records from marine sequences are reliable and useful tools
89 to reconstruct changes in the regional vegetation of adjacent landmasses and the climate dynamics
90 at orbital and suborbital timescales. In arid environments, marine sequences are particularly
91 essential in providing continuous records of vegetation change at the regional scale.

92 The pollen sequence from MD96-2098 presented here covers the period between 24 and
93 *thousand years before present* 190 ka and provides an integrated picture of past regional vegetation changes in southwestern
94 Africa. Southwestern Africa refers here to the western half of South Africa and Namibia that is
95 drained by the Orange River. We compare vegetation-based atmospheric changes with independent
96 climatic markers from the same marine sequence, along with other regional records for oceanic

97 conditions and global ice dynamics, to reconstruct atmospheric and oceanic configurations around
98 southern Africa for MIS 6, 5, 4 and 3.

99

100 2. Modern environmental setting

101 The southwestern part of the African continent (Atlantic side) is influenced by the seasonal
102 migration of the subtropical front and the southern westerlies that bring precipitation during the
103 austral-winter months (Beal et al., 2011). Precipitation in southwestern Africa is additionally
104 controlled by the cold Benguela current and wind-driven upwelling that results in aridity on the
105 adjacent continent (Stuut and Lamy, 2004). In the Indian Ocean, warm waters from the Agulhas
106 current (Beal and Bryden, 1999) and austral-summer heat enhance evaporation and result in
107 relatively high precipitation in southeastern Africa and the interior of the continent (Fig. 1). Austral-
108 summer precipitation is also linked to the position of tropical low pressure systems (e.g. ITCZ) and
109 reduced subtropical high pressure (Tyson and Preston-Whyte, 2000). As tropical low-pressure
110 systems migrate northwards during the austral winter, subtropical high pressure significantly
111 reduces austral-summer precipitation in southern Africa. This climatic configuration broadly
112 determines the vegetation distribution in southern Africa. Phytogeographical regions were initially
113 classified by White (1983), and later revisited and described into seven biome units by Rutherford
114 (1997). These include the Succulent-Karoo, Nama-Karoo, Desert, savanna, Fynbos, Grassland, and
115 forest (Fig. 1). *See also Goldblatt et al 1978*

116 The Succulent-Karoo receives between 20 and 290 mm/yr of which more than 40% falls
117 during the austral-winter months (Rutherford, 1997). The two most abundant succulent families are
118 Crassulaceae and Mesembryanthemaceae, and non-succulents are Anacardiaceae, Asteraceae, and
119 Fabaceae (Milton et al., 1997). C4 perennial grasses (Poaceae) have relatively low abundance in the
120 Succulent-Karoo (Milton et al., 1997).

121 The Nama-Karoo receives precipitation from 60 to 400 mm/yr falling primarily during the
122 austral summer (Palmer and Hoffman, 1997). Vegetation is characterized as dwarf open shrub land

123 with high abundance of Poaceae, Asteraceae, Aizoaceae, Mesembryanthemaceae, Liliaceae and
124 Scrophulariaceae (Palmer and Hoffman, 1997). Grasses from the Poaceae family can be particularly
125 dominant in the Nama-Karoo biome (Fig. 2a). The Nama- and Succulent-Karoo are structurally similar
126 but influenced by different seasonal precipitation (Rutherford, 1997). The Nama-Karoo is influenced
127 primarily by austral summer precipitation, while the distribution of the Succulent-Karoo coincides
128 with the austral-winter rainfall region (Chase and Meadows, 2007). To the northwest, the Nama-
129 Karoo biome transitions into the Desert, where mean annual precipitation can be as low as 20
130 mm/yr (Jurgens et al., 1997). The Desert reaches 300 km inland and its extent is linked to the
131 intensity of BUS (Lutjeharms and Meeuwis, 1987).

See also Barnard, P (ed.) Biological diversity in Namibia, pages 17 and 18 in particular

132 High precipitation seasonality (i.e. difference between dry-season and rainy-season
133 precipitation) and high austral-summer rainfall characterize the savanna. The savanna biome
134 represents a mosaic that includes shrublands, dry forests, lightly-wooded grasslands, and deciduous
135 woodlands (Scholes, 1997). At the landscape scale however, the savanna can be subdivided into the
136 fine- and broad-leaved savannas based on moisture conditions and soils (Scholes, 1997). The fine-
137 leaved savanna (Fn-LSav) is found in dry and fertile environments (between 400 and 800 mm/yr),
138 and the ~~broad-leaved savanna (Bd-LSav)~~ is found in nutrient-poor and moist environments (up to
139 1500 mm/yr) (Scholes, 1997). Additionally, in the Fn-LSav fuel load and fire frequency are very low,
140 while Bd-LSav has high fuel load and fire frequency (Scholes, 1997; Archibald et al., 2010). The Fn-
141 LSav is found to the northeast of the Nama-Karoo biome (Fig. 1), known as the Kalahari Highveld
142 transition zone (Cowling and Hilton-Taylor, 2009). Due to the transitional character of the Fn-LSav,
143 some of its outer parts have been included in the grassland or Nama-Karoo biomes (White, 1983).
144 The composition of the Fn-LSav can be similar to that of the Nama-Karoo, with dominance of C4
145 grasses (Poaceae) and succulent plants, but it differs in having scattered trees (Fig. 2b) (Cowling et
146 al., 1994). The Bd-LSav is characterized by broad-leaved trees from the Caesalpinaceae and
147 Combretaceae families and an understory dominated by grasses (Scholes, 1997).

(no correction)

148 The grassland biome is dominated by C4 grasses and non-grassy forbs as *Anthospermum* sp.,
149 *Lycium* sp., *Solanum* sp. and *Pentzia* sp. (O'Connor and Bredenkamp, 1997). At the high elevations
150 the biome is dominated by C3 grasses. In the grasslands, precipitation is highly seasonal with mean
151 annual rainfall ranging between 750 and over 1200 mm, falling primarily during the austral-summer
152 months (O'Connor and Bredenkamp, 1997) (Fig.1).

153 The southernmost part of Africa is characterised by the Fynbos biome, a fire-prone
154 vegetation dominated by Ericaceous and Asteraceae shrubs, diverse *Protea* shrubs and trees, and
155 Restionaceae herbs (Cowling et al., 1997a). The Fynbos biome receives relatively high annual
156 precipitation (1200 mm per year) concentrated during the austral-winter months (Rutherford, 1997).
157 The coastal forest biome is found along the eastern coast of the subcontinent and often occurs in
158 small patches with high abundance of *Podocarpus* (Rutherford, 1997). *Podocarpus* patches can also
159 be found in the southeastern part of the Fynbos.

160

161 3. Materials and Methods

162 3.1 Marine core description and pollen analysis

163 Pollen analysis was conducted on marine core MD96-2098 (25°36'S, 12°38'E). This giant
164 CALYPSO core was collected during the IMAGES II-NAUSICAA cruise at a 2910-m water depth from
165 the Lüderitz slope in the Walvis Basin, approximately 500 km northwest of the Orange River mouth
166 (Fig.1). The sediments of this 32-m long core were composed of calcium carbonates (foraminifera),
167 biogenic silica (nannofossil mud), clays and organic matter (Bertrand et al., 1996). The core was
168 sampled every 10 cm between 450 and 1940 cm (uncorrected depth) for pollen analysis. The
169 uncorrected depth did not take into account artificial gaps created during piston extraction
170 (Bertrand et al., 1996).

171 Sample volumes were estimated by water displacement. Pollen concentrations per unit
172 volume were calculated based on a known spike of exotic *Lycopodium* spores added to each sample.
173 Pollen extraction techniques included treatment with Hydrofluoric and Hydrochloric acids, and

why a 150 µm filter?

174 sieving through 150 and 10-µm filters. This filtration allowed eliminating small non-palynomorph
175 particles and concentrating pollen grains and spores. An independent test of this protocol showed
176 that the use of a 10-µm sieve had no effect on the pollen ^{spectra} [composition] of marine samples, i.e.
177 comparison of filtered and unfiltered sample counts showed that taxa were not selectively filtered
178 out during pollen preparation and concentration (see [http://www.ephe-
179 paleoclimat.com/ephe/Lab%20Facilities.htm](http://www.ephe-
179 paleoclimat.com/ephe/Lab%20Facilities.htm) for a detailed pollen preparation protocol).

180 We used the pollen spectra from 31 ^{terrestrial} surface samples collected along a transect (Fig.1) from
181 Cape Town (South Africa) to Lüderitz (Namibia) and designed to cover the four major biomes of
182 southwestern Africa (Supplementary-Table1). The transect included samples from the Desert,
183 Fynbos, Nama- and Succulent-Karoo. The samples were treated with standard acetolysis (Faegri and
184 Iversen, 1989) and ^{analysed} scanned under the microscope until ^a [completing] pollen sums ^{of} were greater than
185 300 grains (^{was reached.} Supplementary-Table1). We also used previously-published pollen spectra from 150
186 additional surface samples collected between 22° and 35° latitude south (APD, Gajewski et al. 2002).

187 These pollen spectra were used to assess the distribution of Poaceae pollen percentages and other ^{(expressed as an} pollen taxa
188 ^{by with indicator value} potential indicators of large biomes in southern Africa. ArcGIS 10 was used to draw iso-lines of
189 pollen percentages by interpolating values from a total of 178 surface samples through the natural
190 neighbour method. Additionally, we analysed two marine pollen samples from the upper part of
191 core MD96-2098 (at 5 and 10 cm depth). We compared the pollen spectra from these core top
192 samples with the pollen signal of the modern vegetation to evaluate how well marine sediments
193 represent the vegetation of the adjacent landmasses, and to aid interpretation of the pollen record.

194 Pollen identification was aided by the pollen reference collection of the Department of Plant
195 Sciences at University of the Free State (Bloemfontein, South Africa), the African Pollen Database
196 (APD) (<http://medias3.mediasfrance.org/pollen>), the Universal Pollen Collection
197 (<http://www.palyno.org/pollen>), and pollen descriptions published by (Scott, 1982). Pollen grains
198 from the Asteraceae family were grouped into three pollen taxa: *Artemisia*-type, *Stoebe*-type and
199 other morphotypes were classified into Asteraceae-other. Some morphotypes were grouped into

200 family types: Acanthaceae, Chenopodiaceae-Amaranthaceae, Crassulaceae, Cyperaceae, Ericaceae,
201 Myrtaceae, Ranunculaceae, Restionaceae, and Solanaceae.

202 To summarize changes in the fossil pollen record over time, detrended correspondence
203 analysis (DCA) was used in tandem with non-metric multidimensional scaling (NMDS) as parametric
204 and non-parametric alternatives (McCune and Grace, 2002). Results from the DCA ordination were
205 preferred when NMDS was unable to reach a stable solution after several random starts, and when
206 stress levels were too high to allow a meaningful interpretation (McCune and Grace, 2002). These
207 ordinations were run filtering out pollen morphotypes that only occurred in one sample to avoid
208 overweighting rare taxa.

209

210 3.2 Marine core chronology

211 Two sediment gaps between 693 and 709 cm and 759 and 908 cm were described in the
212 core log. These gaps were considered artificial and linked to piston extraction (Bertrand et al., 1996),
213 thus the record could be assumed continuous. Depths were corrected to take into account the
214 artificial sediment gaps. An age model was established for the record based on 16 marine isotope
215 events (MIE) from the *Cibicides wuellerstorfi* $\delta^{18}\text{O}$ benthic record of MD96-2098 (Bertrand et al.,
216 2002) and 14 Accelerator Mass Spectrometer radiocarbon ages (AMS ^{14}C) from mixed planktonic
217 foraminifera extracted from MD96-2098 (Supplementary-Table1). The 14 AMS ^{14}C dates were
218 produced at the Laboratoire de Mesure du Carbone 14. One single ^{14}C date showed an age reversal
219 and was therefore excluded from the chronology on the principle of parsimony. AMS ^{14}C ages were
220 calibrated using the marine09.14c curve (Hughen et al., 2004) from CALIB REV6.0.0 (Stuiver and
221 Reimer, 1993). We applied a 400-year global reservoir correction factor and a weighted mean Delta
222 R of 157 years derived from 9 regional reservoir error values from the Marine Reservoir Correction
223 Dataset (Dewar et al., 2012;Southon et al., 2002). MIE ages were derived from LR04 global stack
224 (Lisiecki and Raymo, 2005) and additional sources (Henderson and Slowey, 2000;Drysdale et al.,
225 2007;Waelbroeck et al., 2008;Masson-Delmotte et al., 2010;Sanchez Gofñi and Harrison, 2010)

226 (Supplementary-Fig.1) Sample ages were calculated using a linear interpolation between AMS ¹⁴C
227 ages and MIE using the R package PaleoMAS (Correa-Metrio et al., 2010).

228

229 4. Results and discussion

230 4.1 Pollen preservation and sources in marine core MD96-2098

231 Pollen sums excluding spores range from 100 to 240 grains in 141 samples analysed from
232 core MD96-2098. The mean number of taxa per sample was 21. Total pollen concentration ranged
233 between ca. 300 and 16,000 grains/cm³ during most of MIS 6, 5 and 3 and increased up to 48,000
234 grains/cm³ during MIS 4 (Supplementary-Fig.2). The MIS5 pollen concentrations were comparable to
235 those found in other oceanic margins (Sánchez Goñi et al., 1999), even though BUS facilitates
236 preservation of pollen grains and other organic microfossils at this site (Bertrand et al., 2003). The
237 low net primary productivity that characterizes southwestern Africa (Imhoff et al., 2004) could
238 explain relatively low pollen concentrations in the continental margin (Supplementary-Fig.2).

239 Pollen grains are part of the fine sediment fraction and can be transported by two main
240 vectors: aeolian or fluvial (Hooghiemstra et al., 1986; Heusser and Balsam, 1977). Dupont and
241 Wyputta (2003) modelled present-day wind trajectories for marine core locations between 6 and
242 30°S along the coastline of southern Africa. They suggest aeolian pollen input to the Walvis area
243 (23°S) via the south-east trade winds during austral summer, and dominant east-to-west wind
244 directions during the austral fall and winter. These winds transport pollen and other terrestrial
245 particles from the Namib Desert, southern Namibia and western South Africa. The direction of the
246 winds indicate that the Namib Desert, Nama-Karoo and Succulent-Karoo are the most likely sources
247 of pollen in the Walvis area (Dupont and Wyputta, 2003). The authors also infer that south of 25°S
248 wind directions are predominantly west to east and aeolian terrestrial input very low. Marine site
249 MD96-2098 is located less than a degree south of the area determined by Dupont and Wyputta
250 (2003) to be dominated by terrestrial aeolian input. However, given that this threshold was

transported
would be helpful to indicate this area
in Figure 1.

this is in contrast to
the text in lines 184-185.

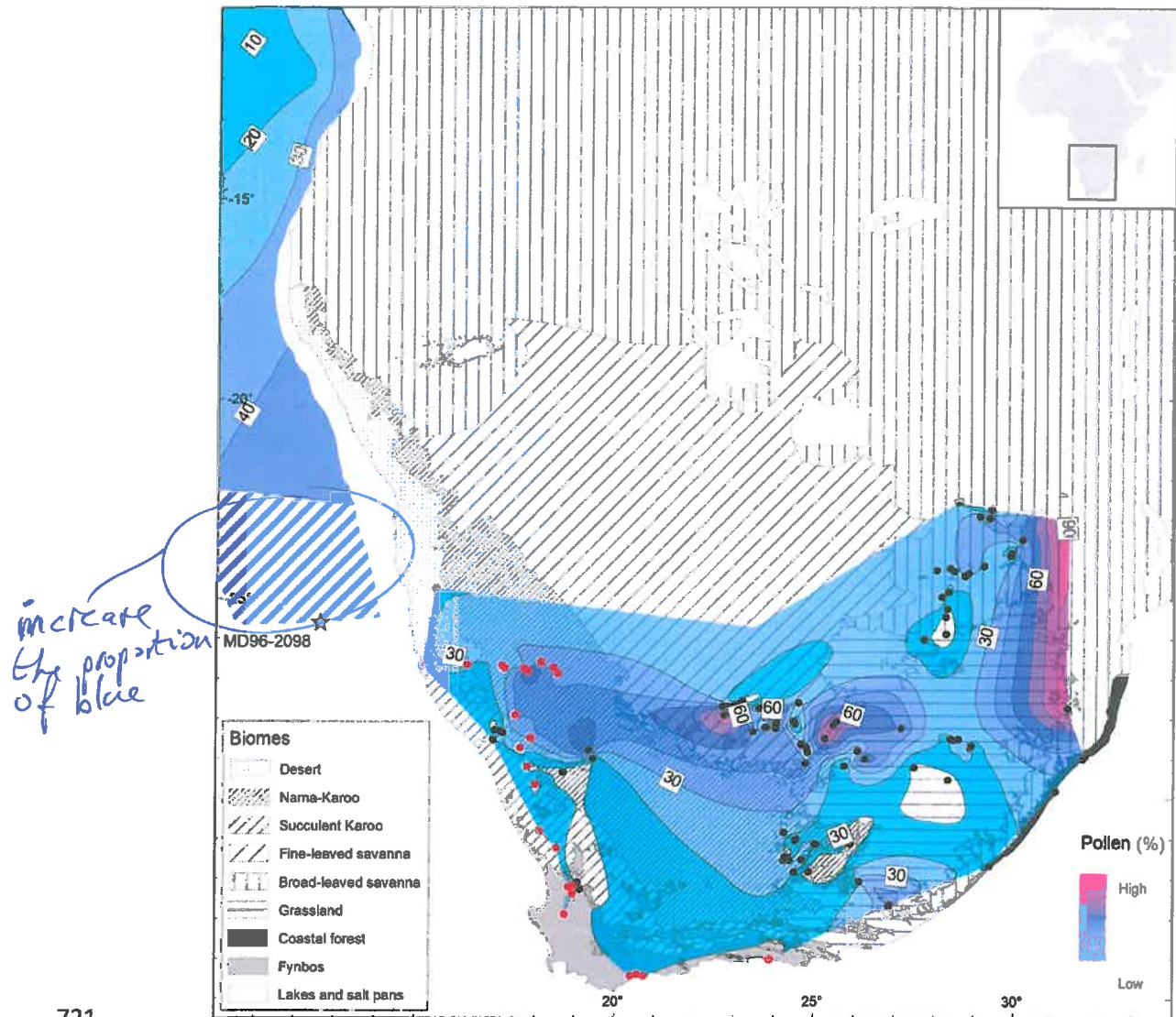
251 established using only two marine sites located 6° apart at 23°26' (GeoB1710-3) and 29°27'
252 (GeoB1722-1), it is difficult to conclude that MD96-2098 only receives wind-transported pollen.

253 MD96-2098 likely receives fine sediments from the Orange River plume. Sedimentological
254 analyses of the Orange River delta and plume indicate that fine muds are transported both
255 northwards and southwards (Rogers and Rau, 2006). Additionally, an analysis of the imprint of
256 terrigenous input in Atlantic surface sediments found relatively high Fe/K values along the Namibian
257 and South African margin that could reflect the input of Orange River material (Govin et al., 2012).
258 Pollen grains are hence likely to reach the coring site from the Orange River catchment area.

259 Scott et al. (2004) argue that pollen in marine sediments can be the result of long-distance
260 transport by ocean currents, suggesting that pollen assemblages in marine sediments do not reflect
261 accurately past changes in vegetation and climate. However, the highest pollen influx in marine
262 sediments along this margin is near the coast and the vegetation source (Dupont et al., 2007), not
263 along the paths of oceanic currents (i.e. Benguela Current). Additionally, analyses of pollen transport
264 vs. source in northwestern Africa show that pollen grains can sink rapidly in the water column
265 (Hooghiemstra et al., 1986) before they can be carried away by ocean currents. As a result, influence
266 of oceanic currents on the composition of pollen assemblages is probably negligible. Overall, the
267 marine site MD96-2098 might receive both aeolian and fluvial pollen input from the vegetation
268 located east and southeast to the site.

269 The pollen ^{spectra} composition of the two core-top samples from core MD96-2098 are dominated
270 by Poaceae (30 and 40%), Cyperaceae (20%) and Chenopodiaceae-Amaranthaceae (20 and 30%)
271 (Supplementary-Fig.2). This composition corresponds well with the pollen spectra from the three
272 major biomes occupying today the adjacent landmasses (Fig.1a): Desert, Nama-Karoo and Fn-LSav
273 (Supplementary-Fig.3 and 5). Pollen percentages from Fynbos taxa are less than 10%, *Podocarpus* is
274 weakly represented, and taxa specifically found in the broad-leaved savanna (e.g. Caesalpinaceae,
275 Combretaceae) are not recorded. These results support the assumption that the main pollen source
276 from marine core MD96-2098 is the vegetation from southwestern Africa.

Suppl Fig Fig. 4 skipped?



721
722
723
724
725
726
727
728
729
730

Figure 3. Poaceae pollen percentage iso-lines drawn over biome units of southern Africa (modified from Scholes (1997); Mucina et al., (2007)). The broad-leaved savanna distribution includes the Mopane and mixed savannas described by Scholes (1997). Iso-lines are plotted based on pollen percentage data from surface samples analysed in this study (red dots) and pollen spectra from other samples previously published and extracted from the African Pollen Database (black dots) (Gajewski et al., 2002). Poaceae pollen percentage in the marine domain are redrawn from Dupont and Wyputta (2003) and extended to latitude 25°S using two MD96-2098 core-top samples (hatched).

277

278 4.2 Distribution and interpretation of Poaceae pollen in terrestrial and marine surface samples

279 Occurrence of Poaceae pollen in all surface samples corresponds to the presence of grass
280 species in virtually all southern African biomes (Cowling et al., 1997b). Altogether, the spatial
281 distribution of Poaceae pollen percentages appears to be essential information to distinguish the
282 pollen signal from major biomes, and therefore climatic zones, in this region. In the eastern and
283 northeastern part of southern Africa, the highest percentages of Poaceae pollen (up to 90%) are
284 found in the pollen rain of the Bd-LSav and grasslands. In the western half of southern Africa,
285 Poaceae pollen percentages in terrestrial surface samples are up to 60% in the Nama-Karoo and its
286 transition with the Fn-LSav (Fig. 3). This suggests an overrepresentation of Poaceae in the pollen rain
287 of the Nama-Karoo biome where grasses can be abundant but are not necessarily dominant.
288 Poaceae is likely to be well represented in other parts of the Fn-LSav, but the paucity of surface
289 samples from this biome hinder drawing further conclusions. In the Namib Desert where ^{proportions} abundance
290 of grasses in the vegetation is low, Poaceae pollen percentages are as high as 25% ^{terrestrial} in surface
291 samples, comparable to 20% reported from hyrax dung (Scott et al., 2004).

292 In marine surface samples along the southwestern African coast, Poaceae pollen
293 percentages are as low as 10% in samples collected ^{offshore} in front of the Bd-LSav at around 15°S (Fig. 3).
294 Poaceae pollen percentages increase to the ^s south and the highest values (40%) are found between
295 20 and 25°S (Dupont and Wyputta, 2003) and correspond well with the distribution of the Desert
296 and the Fn-LSav on the continent. The Poaceae pollen percentages ^{of} from the two core-top samples
297 from MD96-2098 ^{reflecting} dating to the last millennium extend the iso-lines drawn by Dupont and Wyputta
298 (2003) to 25.5°S, and show that Poaceae pollen percentages are between 30 and 40% in front of the
299 Desert, Nama-Karoo and Fn-LSav biomes. As Poaceae pollen percentages in Desert surface samples
300 are less than 25%, high percentages of grass pollen from marine sediments in the southwestern
301 Africa margin should be interpreted as indicator of the Nama-Karoo and the Fn-LSav, where Poaceae

302 is as high as 70% in terrestrial surface samples. Our field observations also support this view as we
303 observed large grass-dominated vegetation in the Nama-Karoo of southern Africa (Fig. 2).

304

305 4.3 Southwestern Africa vegetation and climatic changes from MIS 6 to 2

306 The pollen record presented here spans from 24.7 to 190 ka. A log transformation of
307 concentration values in MD96-2098 results in a curve remarkably similar to that of $\delta^{18}\text{O}_{\text{benthic}}$ values

308 (Fig. 4) and may be linked to changes in pollen input at the coring site. Relative increases in pollen

309 concentration could indicate an increase in pollen ^{supply} arrival during low sea-level stands when the

310 vegetation source was closest (i.e. during glacial stages). However, this is unlikely because of the

311 ^[] width of the Walvis continental Shelf ^{S/ []} (i.e. rapid depth change in a few kilometres). An increase of

312 pollen concentration might indicate instead an increase in aeolian and riverine pollen ^{supply} input during

313 glacials, and/or an increase in pollen preservation linked to upwelling enhancement as suggested by

314 Pichevin et al. (2005). Glacial-interglacial pollen concentration variations have no effect on the

315 interpretation of the pollen record based on relative frequencies, but they do indicate the influence

316 of the obliquity signal in the pollen record from MD96-2098. *In other words the effect of precipitation on the density of the vegetation and the pollen production as a consequence.*

317 The axis scores on DCA1 reveal changes in the composition of pollen assemblages that also

318 resemble variations in the $\delta^{18}\text{O}_{\text{benthic}}$ record (Fig. 4). DCA1 axis scores from MIS 5 and 3 are overall

319 positive in value, while scores from MIS 6 and 4 are negative. A series of large-magnitude changes in

320 DCA1 axis scores (i.e. when adjacent sample scores switch from positive to negative values) are also

321 visible and increase in amplitude after c. 100 ka. Such changes in DCA Axis1 scores are also observed

322 during MIS 6 but are of lesser magnitude. Changes in DCA axis scores suggest significant changes in

323 vegetation composition from one time step to the next (i.e. adjacent samples).

324 Nama-Karoo and Fn-LSav pollen percentages are up to 60% during MIS 5 and display three

325 percentage peaks that correspond with $\delta^{18}\text{O}_{\text{benthic}}$ and precession minima (Fig. 4a). These percentage

326 peaks are centred at 125 ka, 107 and 83 ka. The composition of pollen spectra from warm marine

327 substages MIS 5e, 5c and 5a, is comparable to the core-top samples (Supplementary-Fig. 2). At the

328 same time, the proportion of pollen taxa in these top-core samples corresponds well with the
329 modern pollen spectra from Nama-Karoo and fine-leaved savanna (Supplementary-Fig.3).
330 Additionally, Nama-Karoo and Fn-LSav pollen percentages in last-millennium samples are relatively
331 low compared to their maximum during MIS 5e (Fig.4b). During MIS 6 and 4, Nama-Karoo and Fn-
332 LSav percentages are reduced and co-vary with $\delta^{18}\text{O}_{\text{benthic}}$ values. Pollen percentages of
333 Chenopodiaceae-Amaranthaceae and Asteraceae-other are relatively high and increase along with
334 enriched $\delta^{18}\text{O}_{\text{benthic}}$ values during MIS 6 and at the end of MIS 4 (Supplementary-Fig.2). Cyperaceae *where?*
335 pollen percentages vary importantly throughout the record and are as high as 40% during MIS 4. *down.*
336 Fynbos indicators (Ericaceae, *Passerina*, *Anthospermum*, *Cliffortia*, and *Protea Artemisa*-type and
337 *Stoebe*-type) show relative increases in pollen percentage during MIS 6, 4 and 3 (Fig.4b and
338 Supplementary-Fig.2). Pollen percentages of Restionaceae increase after the 105-ka $\delta^{18}\text{O}_{\text{benthic}}$
339 minimum and remain abundant during the rest of MIS 5 through MIS 3, despite a relative decrease
340 during MIS 4. *Podocarpus* percentages are lower than 10% but show increases at stage boundaries
341 around 135 ka (MIS 6/5), 100 ka (5c/5b), 75 ka (MIS 5a/4), 60 ka (MIS 4/3), and around 27 ka (MIS
342 3/2) (Supplementary-Fig.2).

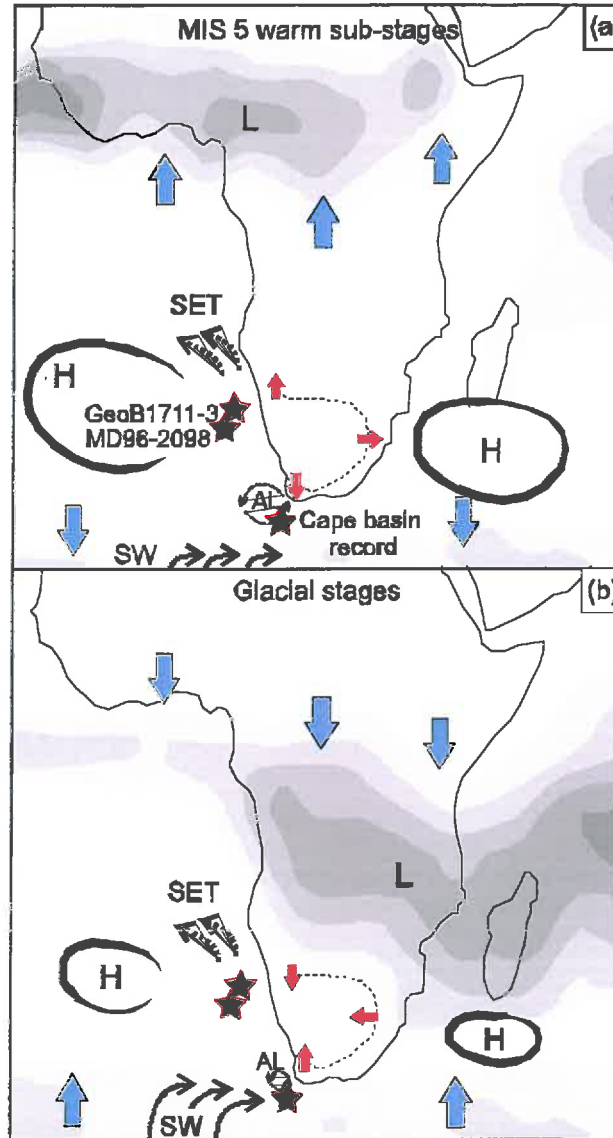
343 The increases of Nama-Karoo and Fn-LSav during MIS 5e, 5c and 5a suggest an increase in
344 aridity in southwestern Africa that likely resulted from expansions in three directions (Fig.5). The
345 Nama-Karoo and Fn-LSav probably expanded to the northwest into the present-day area of the
346 coastal Namib Desert as the intensity of BUS weakened during MIS 5 warm substages. This
347 weakening has been documented through alkenone-based SST from marine core GeoB1711-3 (Kirst
348 et al., 1999) (Fig.4c), foraminifera-assemblage based SST (Chen et al., 2002) and grain-size end-
349 member modelling (Stuut et al., 2002). Stuut and Lamy (2004) also suggested reduced atmospheric
350 circulation and weakening of trade winds during interglacials compared to glacials, resulting in a
351 reduction of the wind-driven upwelling. A weakened BUS and the associated relative increase in
352 humidity likely led to a colonization of Desert areas by Nama-Karoo or Fn-LSav (Fig.5a). Comparable

739
740
741
742
743
744
745
746

number of particles per gram (nb.g^{-1}) from marine core MD96-2098 plotted against age in ka (thousands of calibrated/calendar years before present). Stars on the left correspond to percentage of pollen taxa in two top-core samples dating 530 and 1060 calibrated years before present. (c) Independent climatic records discussed in the text. Gray curve: low-resolution CO_2 record from Vostok (Petit et al. 1999); black curve: high-resolution CO_2 record from Bereiter et al (2012). Stage boundary ages for 3/2, 4/3, and 5/4 from (Sanchez Gofii and Harrison, 2010) and 6/5 from (Henderson and Slowey, 2000).

what is "nb"?

cal



747
748
749
750
751
752
753
754
755
756
757
758
759

Figure 5. Schematic and simplified configuration of vegetation, atmospheric, and oceanic systems over southern Africa during (a) the MIS 5 warm substages, and (b) glacial isotopic stages. Rainfall is illustrated as grey areas showing the current configuration of tropical and subtropical convection systems using average austral-winter (a) and austral-summer (b) precipitation data between 1979–1995 from the International Research Institute for Climate Prediction (<http://iri.ldeo.columbia.edu>). L: tropical low-pressure systems, H: subtropical high-pressure systems, SET: southeast trade winds, SW: southern westerlies, AL: Agulhas leakage. Stars indicate the location of marine records discussed in the text and blue arrows indicate the direction of pressure system migration. Red arrows and brown shaded area indicate hypothesized expansion (a) or contraction of the Nama-Karoo and fine-leaved savanna (b).

353 contractions of the Namib Desert linked to increased SSTs and weakening of BUS during the present
354 interglacial are documented by Shi et al. (2000).

355 To the south, the Nama-Karoo and Fn-LSav likely expanded at the expense of the Succulent-
356 Karoo and Fynbos. Warmer Antarctica temperatures recorded during warm substages of MIS 5 than
357 during MIS 1 (EPICA, 2006) would drive the southern westerlies polewards (Ruddiman, 2006),
358 contributing to the ventilation of deep CO₂-rich waters in the southern Ocean (Toggweiler and
359 Russell, 2008). This mechanism would explain the paralleling trends observed between MIS 5 Nama-
360 Karoo and Fn-LSav expansions in southern Africa and the atmospheric CO₂ record (Petit et al.,
361 1999; Bereiter et al., 2012) (Fig.5). A poleward migration of the westerlies during the present
362 interglacial, relative to their position during the previous glacial period, has been suggested by
363 (Weldeab et al., 2013), and correlated with nssCa²⁺ from Antarctica (Röthlisberger et al., 2008). Such
364 poleward migration of the westerlies during the present interglacial is equivalent to the westerlies
365 migration we propose for warmest periods of the last interglacial. The increased Agulhas leakage
366 documented in the Cape basin record during the last interglacial (Peeters et al., 2004) (Fig.4c) has
367 been linked to a southward migration of the subtropical front and the westerlies, reducing austral-
368 winter precipitation over southern Africa. Such an atmospheric configuration would in turn favour
369 the development of the Nama-Karoo at the expense of Succulent-Karoo and Fynbos biomes (Fig.5a).

370 To the northeast, Nama-Karoo and Fn-LSav likely pushed the limit of Bd-LSav equatorward as
371 austral-summer precipitation decreased (Fig.5a). Austral-summer precipitation reductions in
372 ^Ssouthern Africa have been linked to reduced austral-summer insolation in the Pretoria saltpan
373 (Partridge et al., 1997) and to reductions of grass-fuelled fires during precession minima
374 reconstructed from MD96-2098 (Daniau et al., 2013) (Fig.4b). Increased northern-hemisphere
375 insolation during MIS 5 warm substages would drive the ITCZ northwards while subtropical high
376 pressure cells over the south Atlantic and the Indian Oceans would expand (Fig.5a) (Ruddiman,
377 2006). Such changes in the tropical and subtropical pressure systems would allow the expansion of
378 the Nama-Karoo and Fn-LSav to the northeast.

379 In contrast with the results presented here, previous studies report poleward interglacial
380 expansions of savannas based on pollen records from marine sediments along the southwestern
381 African coast (Dupont, 2011). However, these studies univocally interpret the Poaceae pollen
382 percentage increases as the result of savanna expansions. Such an interpretation is potentially
383 plausible in marine records collecting pollen from broad-leaved savanna vegetation, e.g. the
384 Limpopo basin (Dupont et al., 2010a). However, our study shows that Poaceae pollen percentage
385 increases in sequences located off the southwestern African coast ~~can~~ ^{may be indicative of} alternatively indicate the
386 expansion of fine-leaved savanna and Nama-Karoo vegetation. These previous studies do not
387 differentiate between the ~~broad-leaved~~ ^{Bd-LSav} and ~~fine-leaved savannas~~ ^{Fn-LSav}, despite the significant climatic
388 and structural differences between these two types of vegetation. The Bd-LSav is influenced by fire
389 and receives a considerable amount of precipitation during the austral summer (Scholes, 1997). The
390 Fn-LSav is structurally and climatically more similar to the Nama-Karoo biome, as it receives very low
391 austral-summer precipitation and does not burn (Archibald et al., 2010) despite being under a
392 regime of significant precipitation seasonality (Scholes, 1997). If high Poaceae pollen percentages
393 during MIS 5 warm substages in our record were related with expansions of the Bd-LSav and
394 increased summer precipitation, the fire activity should also increase during these substages.
395 Instead, an independent charcoal record from the same marine sequence MD96-2098 (Fig.4b)
396 documents reductions of grass-fuelled fires and a decrease in austral-summer precipitation during
397 MIS5 precession minima (Daniau et al., 2013). An atmospheric configuration with reduced austral
398 summer precipitation in ~~s~~ southern Africa and the ITCZ shifted northward during the warmest periods
399 of MIS 5 is also consistent with documented strengthening of Asian monsoon and weakening of the
400 South American monsoon during the last-interglacial precession minima (Wang et al., 2004).

401 Our results suggest that the Bd-LSav retreated equatorwards during MIS 5 precession
402 minima, while Nama-Karoo and Fn-LSav expanded. Nama-Karoo and Fn-LSav probably covered a
403 surface area larger than at present during MIS 5 warm substages, as indicated by up to 70% pollen
404 from this biome during MIS 5 compared to 35% in the core-top samples. This is despite the

or "southern African" ?
check the area considered

405 difference in precession parameters between the last millennium and MIS 5 warm substages. Recent
406 model experiments on the impact of precession changes on South African vegetation indicate that
407 high precession is linked to reductions of the ^{Bd-LSav} ~~broad-leaved savannas~~ (Woillez et al., 2014).
408 Altogether these vegetation changes point to increased aridity in southwestern Africa during the
409 warmest periods of the last interglacial.

410 During glacial isotopic stages, contractions of the Nama-Karoo and Fn-LSav would result
411 from a different atmospheric configuration (Fig.5b): a southward migration of the ITCZ and the
412 associated South African monsoon (Daniau et al., 2013; Partridge et al., 1997) increasing austral-
413 summer rainfall over southern Africa; an intensification of BUS and decreased SST off the Namibian
414 coast (Stuut and Lamy, 2004; Kirst et al., 1999) leading to aridification of coastal areas; and lastly, an
415 equatorward migration of the westerlies increasing austral-winter precipitation and allowing a
416 northward expansion of the winter-rain zone in ^{S/} southern Africa (Chase and Meadows, 2007). The ^{see} ^{pages} ⁵ ^{for}
417 proposed glacial precipitation changes are consistent with recent estimates of Last Glacial Maximum ^{consistency}
418 palaeoprecipitation based on glacier reconstruction and mass-balance modelling (Mills et al., 2012),
419 with leaf-wax reconstructions of hydroclimate (Collins et al., 2014), and with simulated glacial
420 climatic fluctuations in southern Africa (Huntley et al., 2014).

421 The pollen record from MD96-2098 also suggested glacial expansions of Fynbos (Fig.4b), as
422 pollen percentages of *Artemisia*-type, *Stoebe*-type, *Passerina* and Ericaceae were higher during MIS
423 6, 4 and 3 than in the core-top samples (Supplementary-Fig.2). These results were consistent with
424 glacial northward expansions of Fynbos documented in other pollen records from southern Africa
425 (Shi et al., 2000; Dupont et al., 2007). Our record also documented a large peak in Fynbos indicators
426 (Fig.4b) that coincided with a fast decrease in Nama-Karoo and fine-leaved savanna pollen
427 percentages at the MIS 5e/5d transition (c. 117 ka), a precession and eccentricity maxima (Laskar,
428 1990), and an accelerated cooling in Antarctica (EPICA, 2006; Masson-Delmotte et al., 2010) (Fig.4c).
429 As pollen percentages of *Artemisia*-type obtained from surface samples were associated with the
430 Fynbos biome and austral-winter precipitation (Supplementary-Fig.4 and 5), it cannot be discarded

431 that this resulted from a rapid and short-lived expansion of the winter-rain zone of southern Africa.
432 Transitions MIS 6/5 and 4/3 were characterized by small but rapid increases in *Podocarpus*,
433 potentially linked to a short increase in annual precipitation. Such increases in *Podocarpus* have also
434 been documented in other records from southern Africa (Dupont et al., 2010b; Dupont, 2011).

435 ? Finally, the amplitude of millennial-scale vegetation changes increased between ca. 100^{ka} and
436 ca. 25 ka, and was highlighted by switches from negative to positive DCA1 scores (Fig. 4b) and increased
437 variability of Restionaceae pollen percentages. These results could indicate either enhanced trade-
438 wind variability or Fynbos vegetation expansions. Other Fynbos indicators did not display such trend
439 (Fig. 4), suggesting that Restionaceae variability between 100^{ka} and 24 ka were more likely the result
440 of enhanced variability of southeast trade winds. Restionaceae pollen percentage data from a record
441 [2 degrees of latitude north / 2° North] of our marine site also showed increased amplitude of millennial-scale changes (Shi et al.,
442 2001). Grain-size wind strength tracers from the Walvis Ridge displayed enhanced millennial-scale
443 variability, although only after ca. 80 ka (Stuut et al., 2002). An analysis of BUS dynamics over the
444 past 190 ka found increased millennial-scale variability of wind strength after ca. 100 ka and the ^{highest}
445 [windiest conditions] in this zone during MIS 4 and 3 (Stuut et al., 2002). Such millennial-scale ^{wind vigor}
446 atmospheric reorganisations are recorded in the pollen-based DCA analysis as rapid biome shifts in
447 southwestern Africa.

448

449 5. Conclusions

450 Terrestrial and marine markers from the marine core MD96-2098 documented expansions
451 of the Nama-Karoo and fine-leaved savanna during MIS 5e, 5c and 5a warm substages.
452 Northwestern expansions of the Nama-Karoo and Fn-LSav are potentially linked to the reduction of
453 BUS and a local increase in humidity in the desert area, while aridification increased at a regional
454 scale. Towards the east, Nama-Karoo and Fn-LSav expansions probably resulted from increased
455 subtropical high pressure, a northward shift of the ITCZ, and reduced austral-summer precipitation.
456 Nama-Karoo and Fn-LSav expansions to the southern boundary are possibly associated with

457 southern displacement of the westerlies and the subtropical front, decreasing austral-winter
458 precipitation.

459 During glacial isotopic stages MIS 6, 4 and 3, Fynbos biome expansions are probably linked
460 to the increased influence of the southern westerlies and austral-winter precipitation in
461 southwestern Africa. Our pollen record also suggested that warm-cold or cold-warm transitions
462 between isotopic stages and substages were punctuated by short increases in humidity. Increased
463 variability of vegetation changes at millennial timescales ca. 100 ka was also documented and could
464 be associated with previously-identified enhanced variability of the southeastern trade winds.

465 Interglacial-glacial southern Africa biome dynamics were linked to atmospheric and oceanic
466 dynamics resulting from changes in global ice volume and precession at orbital timescales.
467 Atmospheric configurations with westerly winds shifted southwards relative to today have been
468 suggested for other interglacials (Peeters et al., 2004) and are projected for the end of 21st-century
469 under current global warming (Beal et al., 2011). This is likely to reduce austral-winter precipitation
470 over southern Africa and favour expansions of the Nama-Karoo at the expense of the winter-rain fed
471 Fynbos and Succulent-Karoo biomes. However, taking the current orbital configuration alone, the
472 Nama-Karoo and Fn-LSav in southern Africa might naturally remain relatively reduced for several
473 millennial ahead.

474

475 **Acknowledgements**

476 We are grateful to Professor L. Scott for giving us access to the pollen reference collection at
477 the University of the Free State, Bloemfontein, South Africa. We also thank Professor K. Gajewski
478 and the African Pollen Database for complementary surface data. We acknowledge the Artemis
479 program for support for radiocarbon dates at the Laboratoire de Mesure du Carbone 14. We thank
480 Murielle Georget and Marie H el ene Castera for sample preparation and pollen extraction, Linda
481 Rossignol for foraminifera preparation for ¹⁴C dating, Ludovic Devaux for help with the surface-
482 sample dataset, and Will Banks for English proof reading. The marine core was retrieved during

483 NAUSICAA oceanographic cruise (IMAGES II). This work was funded by the European Research
484 Council Grant TRACSYMBOLS n°249587 <http://tracsymbols.eu/>.

485

486 **References**

- 487 Archibald, S., Scholes, R. J., Roy, D. P., Roberts, G., and Boschetti, L.: Southern African fire regimes as
488 revealed by remote sensing, *International Journal of Wildland Fire*, 19, 861-878,
489 <http://dx.doi.org/10.1071/WF10008>, 2010.
- 490 Beal, L. M., and Bryden, H. L.: The velocity and vorticity structure of the Agulhas Current at 32°S,
491 *Journal of Geophysical Research: Oceans*, 104, 5151-5176, 10.1029/1998jc900056, 1999.
- 492 Beal, L. M., De Ruijter, W. P. M., Biastoch, A., and Zahn, R.: On the role of the Agulhas system in
493 ocean circulation and climate, *Nature*, 472, 429-436, 10.1038/nature09983, 2011.
- 494 Bereiter, B., Lüthi, D., Siegrist, M., Schüpbach, S., Stocker, T. F., and Fischer, H.: Mode change of
495 millennial CO₂ variability during the last glacial cycle associated with a bipolar marine carbon
496 seesaw, *Proceedings of the National Academy of Sciences*, 109, 9755-9760,
497 10.1073/pnas.1204069109, 2012.
- 498 Bertrand, P., Balut, Y., Schneider, R., Chen, M. T., Rogers, J., and Shipboard Scientific Party: Scientific
499 report of the NAUSICAA-IMAGES II coring cruise. Les rapports de campagne à la mer à bord du
500 Marion-Dufresne, URA CNRS 197, Université Bordeaux1, Département de Géologie et
501 Oceanographie, Talence, France, 382 pp, 1996.
- 502 Bertrand, P., Giraudeau, J., Malaize, B., Martinez, P., Gallinari, M., Pedersen, T. F., Pierre, C., and
503 Vénec-Peyré, M. T.: Occurrence of an exceptional carbonate dissolution episode during early
504 glacial isotope stage 6 in the Southeastern Atlantic, *Marine Geology*, 180, 235-248,
505 10.1016/s0025-3227(01)00216-x, 2002.
- 506 Bertrand, P., Pedersen, T. F., Schneider, R., Shimmiel, G., Lallier-Verges, E., Disnar, J. R., Massias, D.,
507 Villanueva, J., Tribovillard, N., Huc, A. Y., Giraud, X., Pierre, C., and Vénec-Peyre, M.-T.: Organic-
508 rich sediments in ventilated deep-sea environments: Relationship to climate, sea level, and
509 trophic changes, *Journal of Geophysical Research*, 108, 3045, 10.1029/2000JC000327, 2003.
- 510 Biastoch, A., Böning, C. W., and Lutjeharms, J. R. E.: Agulhas leakage dynamics affects decadal
511 variability in Atlantic overturning circulation, *Nature*, 456, 489-492, 2008.
- 512 Chase, B. M., and Meadows, M. E.: Late Quaternary dynamics of southern Africa's winter rainfall
513 zone, *Earth-Science Reviews*, 84, 103-138, <http://dx.doi.org/10.1016/j.earscirev.2007.06.002>,
514 2007.
- 515 Chen, M.-T., Chang, Y.-P., Chang, C.-C., Wang, L.-W., Wang, C.-H., and Yu, E.-F.: Late Quaternary sea-
516 surface temperature variations in the southeast Atlantic: a planktic foraminifer faunal record of
517 the past 600 000 yr (IMAGES II MD962085), *Marine Geology*, 180, 163-181, 10.1016/s0025-
518 3227(01)00212-2, 2002.
- 519 Collins, J. A., Schefuß, E., Govin, A., Mulitza, S., and Tiedemann, R.: Insolation and glacial–interglacial
520 control on southwestern African hydroclimate over the past 140 000 years, *Earth and Planetary
521 Science Letters*, 398, 1-10, <http://dx.doi.org/10.1016/j.epsl.2014.04.034>, 2014.
- 522 Cowling, R. M., Esler, K. J., Midgley, G. F., and Honig, M. A.: Plant functional diversity, species
523 diversity and climate in arid and semi-arid southern Africa, *Journal of Arid Environments*, 27,
524 141-158, 1994.
- 525 Cowling, R. M., Richardson, D. M., and Mustart, P. J.: Fynbos, in: *Vegetation of Southern Africa*,
526 edited by: Cowling, R. M., Richardson, D. M., and Pierce, S. M., Cambridge University Press,
527 Cambridge, UK, 99-130, 1997a.

the ~80 "and"s could be omitted in this list of references

- 528 Cowling, R. M., and Hilton-Taylor, C.: Phytogeography, flora and endemism, in: The Karoo. Ecological
529 Patterns and Processes, edited by: Dean, W. R. J., and Milton, S., Cambridge University Press,
530 Cambridge, UK, 42-56, 2009.
- 531 Daniau, A.-L., Sánchez Goñi, M. F., Martinez, P., Urrego, D. H., Bout-Roumazelles, V., Desprat, S., and
532 Marlon, J. R.: Orbital-scale climate forcing of grassland burning in southern Africa, Proceedings
533 of the National Academy of Sciences, 110, 5069–5073, 10.1073/pnas.1214292110, 2013.
- 534 Dewar, G., Reimer, P. J., Sealy, J., and Woodborne, S.: Late-Holocene marine radiocarbon reservoir
535 correction (ΔR) for the west coast of South Africa, The Holocene,
536 10.1177/0959683612449755, 2012.
- 537 Drysdale, R. N., Zanchetta, G., Hellstrom, J. C., Fallick, A. E., McDonald, J., and Cartwright, I.:
538 Stalagmite evidence for the precise timing of North Atlantic cold events during the early last
539 glacial, Geology, 35, 77-80, 2007.
- 540 Dupont, L., and Behling, H.: Land–sea linkages during deglaciation: High-resolution records from the
541 eastern Atlantic off the coast of Namibia and Angola (ODP site 1078), Quaternary International,
542 148, 19-28, 10.1016/j.quaint.2005.11.004, 2006.
- 543 Dupont, L., Caley, T., Malaizé, B., and Giraudeau, J.: Patterns of glacial-interglacial vegetation and
544 climate variability in eastern South Africa, EGU General Assembly Conference Abstracts, 2010a,
545 3892, *gray literature still not published?*
- 546 Dupont, L.: Orbital scale vegetation change in Africa, Quaternary Science Reviews, 30, 3589-3602,
547 10.1016/j.quascirev.2011.09.019, 2011.
- 548 Dupont, L. M., Jahns, S., Marret, F., and Ning, S.: Vegetation change in equatorial West Africa: time-
549 slices for the last 150 ka, Palaeogeography, Palaeoclimatology, Palaeoecology, 155, 95-122,
550 10.1016/s0031-0182(99)00095-4, 2000.
- 551 Dupont, L. M., and Wyputta, U.: Reconstructing pathways of aeolian pollen transport to the marine
552 sediments along the coastline of SW Africa, Quaternary Science Reviews, 22, 157-174, 2003.
- 553 Dupont, L. M., Behling, H., Jahns, S., Marret, F., and Kim, J.-H.: Variability in glacial and Holocene
554 marine pollen records offshore from west southern Africa, Vegetation History and
555 Archaeobotany, 16, 87-100, 10.1007/s00334-006-0080-8, 2007.
- 556 Dupont, L. M., Caley, T., Kim, J. H., Castañeda, I., Malaizé, B., and Giraudeau, J.: Glacial-interglacial
557 vegetation dynamics in South Eastern Africa coupled to sea surface temperature variations in
558 the Western Indian Ocean, Climate of the Past, 7, 1209-1224, 10.5194/cp-7-1209-2011, 2010b.
- 559 EPICA: One-to-one coupling of glacial climate variability in Greenland and Antarctica, Nature, 444,
560 195-198, 10.1038/nature05301, 2006.
- 561 Faegri, K., and Iversen, J.: Textbook of Pollen Analysis, 4th ed., Wiley, Chichester, 328 pp., 1989.
- 562 González, C., and Dupont, L. M.: Tropical salt marsh succession as sea-level indicator during Heinrich
563 events, Quaternary Science Reviews, 10.1016/j.quascirev.2008.12.023, 2009.
- 564 Govin, A., Holzwarth, U., Heslop, D., Ford Keeling, L., Zabel, M., Mulitza, S., Collins, J. A., and Chiessi,
565 C. M.: Distribution of major elements in Atlantic surface sediments (36 N–49 S): Imprint of
566 terrigenous input and continental weathering, Geochemistry, Geophysics, Geosystems, 13, 2012.
- 567 Henderson, G. M., and Slowey, N. C.: Evidence from U-Th dating against Northern Hemisphere
568 forcing of the penultimate deglaciation, Nature, 404, 61-66, 10.1038/35003541, 2000.
- 569 Heusser, L., and Balsam, W. L.: Pollen distribution in the northeast Pacific Ocean, Quaternary
570 Research, 7, 45-62, 10.1016/0033-5894(77)90013-8, 1977.
- 571 Hooghiemstra, H., Agwu, C. O. C., and Beug, H.-J.: Pollen and spore distribution in recent marine
572 sediments: a record of NW-African seasonal wind patterns and vegetation belts., Meteor
573 Forschungs-Ergebnisse C, 40, 87-135, 1986.
- 574 Hooghiemstra, H., Stalling, H., Agwu, C. O. C., and Dupont, L. M.: Vegetational and climatic changes
575 at the northern fringe of the Sahara 250,000–5000 years BP: evidence from 4 marine pollen
576 records located between Portugal and the Canary Islands, Review of Palaeobotany and
577 Palynology, 74, 1-53, 10.1016/0034-6667(92)90137-6, 1992.
- 578 Hughen, K., Baillie, M., Bard, E., Bayliss, A., Beck, J., Bertrand, C., Blackwell, P., Buck, C., Burr, G.,
579 Cutler, K., Damon, P., Edwards, R., Fairbanks, R., Friedrich, M., Guilderson, T., Kromer, B.,

- 580 McCormac, F., Manning, S., Ramsey, C. B., Reimer, P., Reimer, R., Remmele, S., Southon, J.,
581 Stuiver, M., Talamo, S., Taylor, F., Plicht, J. v. d., and Weyhenmeyer, C.: Marine04 Marine
582 radiocarbon age calibration, 26 - 0 ka BP, *Radiocarbon*, 46, 1059-1086, 2004.
- 583 Huntley, B., Midgley, G. F., Barnard, P., and Valdes, P. J.: Suborbital climatic variability and centres of
584 biological diversity in the Cape region of southern Africa, *Journal of Biogeography*, 2014.
- 585 Imhoff, M. L., Bounoua, L., Ricketts, T., Loucks, C., Harriss, R., and Lawrence, W. T.: Global patterns in
586 human consumption of net primary production, *Nature*, 429, 870-873, 2004.
- 587 Jürgens, N., Burke, A., Seely, M. K., and Jacobson, K. M.: Desert, in: *Vegetation of Southern Africa*,
588 edited by: Cowling, R. M., Richardson, D. M., and Pierce, S. M., Cambridge University Press,
589 Cambridge, 189-214, 1997.
- 590 Kirst, G. J., Schneider, R. R., Müller, P. J., von Storch, I., and Wefer, G.: Late Quaternary ^ETemperature
591 ^Variability in the Benguela Current System Derived from ^UAlkenones, *Quaternary Research*, 52,
592 92-103, 10.1006/qres.1999.2040, 1999.
- 593 Laskar, J.: The chaotic motion of the solar system: A numerical estimate of the chaotic zones, *Icarus*,
594 88, 266-291, 1990.
- 595 Leroy, S., and Dupont, L.: Development of vegetation and continental aridity in northwestern Africa
596 during the Late Pliocene: the pollen record of ODP site 658, *Palaeogeography,*
597 *Palaeoclimatology, Palaeoecology*, 109, 295-316, 10.1016/0031-0182(94)90181-3, 1994.
- 598 Lisiecki, L. E., and Raymo, M. E.: A Pliocene-Pleistocene stack of 57 globally distributed benthic d18O
599 records, *Paleoceanography*, 20, PA1003, 10.1029/2004pa001071, 2005.
- 600 Lutjeharms, J. R. E., and Meeuwis, J. M.: The extent and variability of South-East Atlantic upwelling,
601 *South African Journal of Marine Science*, 5, 51-62, 10.2989/025776187784522621, 1987.
- 602 Lyle, M., Heusser, L., Ravelo, C., Yamamoto, M., Barron, J., Diffenbaugh, N. S., Herbert, T., and
603 Andreasen, D.: Out of the tropics: the Pacific, Great Basin Lakes, and Late Pleistocene water
604 cycle in the western United States ^SScience, 337, 1629-1633, 2012.
- 605 Masson-Delmotte, V., Stenni, B., Pol, K., Braconnot, P., Cattani, O., Falourd, S., Kageyama, M., Jouzel,
606 J., Landais, A., Minster, B., Barnola, J. M., Chappellaz, J., Krinner, G., Johnsen, S., ^RThlisberger,
607 R., Hansen, J., Mikolajewicz, U., and Otto-Bliesner, B.: EPICA Dome C record of glacial and
608 interglacial intensities, *Quaternary Science Reviews*, 29, 113-128, 2010.
- 609 McCune, B., and Grace, J. B.: ^EAnalysis of ^SEcological ^CCommunities, ^{MjM}MjM, Gleneden Beach, Oregon,
610 300 pp., 2002.
- 611 Meadows, M. E., Chase, B. M., and Seliane, M.: Holocene palaeoenvironments of the Cederberg and
612 Swartuggens mountains, Western Cape, South Africa: Pollen and stable isotope evidence from
613 hyrax dung middens, *Journal of Arid Environments*, 74, 786-793,
614 <http://dx.doi.org/10.1016/j.jaridenv.2009.04.020>, 2010.
- 615 Mills, S. C., Grab, S. W., Rea, B. R., Carr, S. J., and Farrow, A.: Shifting westerlies and precipitation
616 patterns during the Late Pleistocene in southern Africa determined using glacier reconstruction
617 and mass balance modelling, *Quaternary Science Reviews*, 55, 145-159,
618 <http://dx.doi.org/10.1016/j.quascirev.2012.08.012>, 2012.
- 619 Milton, S. J., Yeaton, R. I., Dean, W. R. J., and Vlok, J. H. J.: Succulent karoo, in: *Vegetation of*
620 *Southern Africa*, edited by: Cowling, R. M., Richardson, D. M., and Pierce, S. M., Cambridge
621 University Press, Cambridge, 131-166, 1997.
- 622 O'Connor, T. G., and Bredenkamp, G. J.: Grassland, in: *Vegetation of Southern Africa*, edited by:
623 Cowling, R. M., Richardson, D. M., and Pierce, S. M., Cambridge University Press, Cambridge, UK,
624 215-257, 1997.
- 625 Palmer, A. R., and Hoffman, M. T.: Nama-Karoo, in: *Vegetation of Southern Africa*, edited by:
626 Cowling, R. M., Richardson, D. M., and Pierce, S. M., Cambridge University Press, Cambridge, 167-
627 188, 1997.
- 628 Partridge, T. C., Demenocal, P. B., Lorentz, S. A., Paiker, M. J., and Vogel, J. C.: Orbital forcing of
629 climate over South Africa: A 200,000-year rainfall record from the pretoria saltpan, *Quaternary*
630 *Science Reviews*, 16, 1125-1133, [http://dx.doi.org/10.1016/S0277-3791\(97\)00005-X](http://dx.doi.org/10.1016/S0277-3791(97)00005-X), 1997.

- 631 Peeters, F. J. C., Acheson, R., Brummer, G.-J. A., de Ruijter, W. P. M., Schneider, R. R., Ganssen, G. M.,
632 Ufkes, E., and Kroon, D.: Vigorous exchange between the Indian and Atlantic oceans at the end
633 of the past five glacial periods, *Nature*, 430, 661-665, 10.1038/nature02785, 2004.
- 634 Petit, J. R., Jouzel, J., Raynaud, D., Barkov, N. I., Barnola, J.-M., Basile, I., Bender, M., and Chappellaz,
635 J.: Climate and atmospheric history of the past 420,000 years from the Vostok ice core,
636 Antarctica, *Nature*, 399, 429-436, 1999.
- 637 Pichevin, L., Martinez, P., Bertrand, P., Schneider, R., Giraudeau, J., and Emeis, K.: Nitrogen cycling on
638 the Namibian shelf and slope over the last two climatic cycles: Local and global forcings,
639 *Paleoceanography*, 20, PA2006, 10.1029/2004pa001001, 2005.
- 640 Rogers, J., and Rau, A. J.: Surficial sediments of the wave-dominated Orange River Delta and the
641 adjacent continental margin off south-western Africa, *African Journal of Marine Science*, 28, 511-
642 524, 10.2989/18142320609504202, 2006.
- 643 Röthlisberger, R., Mudelsee, M., Bigler, M., De Angelis, M., Fischer, H., Hansson, M., Lambert, F.,
644 Masson-Delmotte, V., Sime, L., and Udisti, R.: The Southern Hemisphere at glacial terminations:
645 insights from the Dome C ice core, *Climate of the Past*, 4, 345-356, 2008.
- 646 Ruddiman, W. F.: Orbital changes and climate, *Quaternary Science Reviews*, 25, 3092-3112, 2006.
- 647 Rutherford, M. C.: Categorization of biomes, in: *Vegetation of Southern Africa*, edited by: Cowling, R.
648 M., Richardson, D. M., and Pierce, S. M., Cambridge University Press, Cambridge, UK, 1997. pp 91-98
- 649 Sánchez Goñi, M. a. F., Turon, J.-L., Eynaud, F., and Gendreau, S.: European Climatic Response to
650 Millennial-Scale Changes in the Atmosphere-Ocean System during the Last Glacial Period,
651 *Quaternary Research*, 54, 394-403, 10.1006/qres.2000.2176, 2000.
- 652 Sanchez Goñi, M. F., and Harrison, S. P.: Millennial-scale climate variability and vegetation changes
653 during the Last Glacial: Concepts and terminology, *Quaternary Science Reviews*, 29, 2823-2827,
654 2010.
- 655 Sánchez Goñi, M. F., Eynaud, F., Turon, J. L., and Shackleton, N. J.: High resolution palynological
656 record off the Iberian margin: direct land-sea correlation for the Last Interglacial complex, *Earth
657 and Planetary Science Letters*, 171, 123-137, 10.1016/s0012-821x(99)00141-7, 1999.
- 658 Scholes, R. J.: Savanna, in: *Vegetation of Southern Africa*, edited by: Cowling, R. M., Richardson, D.
659 M., and Pierce, S. M., Cambridge University Press, Cambridge, UK, 258-277, 1997.
- 660 Scott, L.: Late Quaternary fossil pollen grains from the Transvaal, South Africa, *Review of
661 Palaeobotany and Palynology*, 36, 241-268, 1982.
- 662 Scott, L., Marais, E., and Brook, G. A.: Fossil hyrax dung and evidence of Late Pleistocene and
663 Holocene vegetation types in the Namib Desert, *Journal of Quaternary Science*, 19, 829-832,
664 10.1002/jqs.870, 2004.
- 665 Scott, L., Neumann, F. H., Brook, G. A., Bousman, C. B., Norström, E., and Metwally, A. A.: Terrestrial
666 fossil-pollen evidence of climate change during the last 26 thousand years in Southern Africa,
667 *Quaternary Science Reviews*, 32, 100-118, <http://dx.doi.org/10.1016/j.quascirev.2011.11.010>,
668 2012.
- 669 Shi, N., Dupont, L. M., Beug, H.-J., and Schneider, R.: Correlation between Vegetation in
670 Southwestern Africa and Oceanic Upwelling in the Past 21,000 Years, *Quaternary Research*, 54,
671 72-80, 10.1006/qres.2000.2145, 2000.
- 672 Shi, N., Schneider, R., Beug, H.-J., and Dupont, L. M.: Southeast trade wind variations during the last
673 135 kyr: evidence from pollen spectra in eastern South Atlantic sediments, *Earth and Planetary
674 Science Letters*, 187, 311-321, 10.1016/s0012-821x(01)00267-9, 2001.
- 675 Southon, J., Kashgarian, M., Fontugne, M., Metivier, B., and Yim, W. W.-S.: Marine reservoir
676 corrections for the Indian Ocean and Southeast Asia, *Radiocarbon* 44, 167-180, 2002.
- 677 Stuiver, M., and Reimer, P. J.: Extended 14C database and revised CALIB radiocarbon calibration
678 program, *Radiocarbon*, 35, 215-230, 1993.
- 679 Stuut, J.-B. W., Prins, M. A., Schneider, R. R., Weltje, G. J., Jansen, J. H. F., and Postma, G.: A 300-kyr
680 record of aridity and wind strength in southwestern Africa: inferences from grain-size

- 681 distributions of sediments on Walvis Ridge, SE Atlantic, *Marine Geology*, 180, 221-233,
682 10.1016/s0025-3227(01)00215-8, 2002.
- 683 Stuut, J.-B. W., and Lamy, F.: Climate variability at the southern boundaries of the Namib
684 (southwestern Africa) and Atacama (northern Chile) coastal deserts during the last 120,000 yr,
685 *Quaternary Research*, 62, 301-309, <http://dx.doi.org/10.1016/j.yqres.2004.08.001>, 2004.
- 686 Toggweiler, J. R., and Russell, J.: Ocean circulation in a warming climate, *Nature*, 451, 286-288, 2008.
- 687 Tyson, P. D.: Atmospheric circulation changes and palaeoclimates of southern Africa, *South African*
688 *Journal of Science*, 95, 194-201, 1999.
- 689 Tyson, P. D., and Preston-Whyte, R. A.: The weather and climate of southern Africa, Oxford
690 University Press Southern Africa, Cape Town, 396 pp., 2000.
- 691 Waelbroeck, C., Frank, N., Jouzel, J., Parrenin, F., Masson-Delmotte, V., and Genty, D.: Transferring
692 radiometric dating of the last interglacial sea level high stand to marine and ice core records,
693 *Earth and Planetary Science Letters*, 265, 183-194, 2008.
- 694 Wang, X., Auler, A. S., Edwards, R. L., Cheng, H., Cristalli, P. S., Smart, P. L., Richards, D. A., and Shen,
695 C.-C.: Wet periods in northeastern Brazil over the past 210 kyr linked to distant climate
696 anomalies, *Nature*, 432, 740-743, 2004.
- 697 Weldeab, S., Stuut, J.-B. W., Schneider, R. R., and Siebel, W.: Holocene climate variability in the
698 winter rainfall zone of South Africa, *Climate of the Past*, 9, 2347-2364, 10.5194/cp-9-2347-2013,
699 2013.
- 700 White, F.: The vegetation of Africa: a descriptive memoir to accompany the Unesco/AETFAT/UNSO
701 vegetation map of Africa, Paris, 356, 1983.
- 702 Woillez, M. N., Levavasseur, G., Daniau, A. L., Kageyama, M., Urrego, D. H., Sánchez-Goñi, M. F., and
703 Hanquiez, V.: Impact of precession on the climate, vegetation and fire activity in southern Africa
704 during MIS4, *Clim. Past*, 10, 1165-1182, 10.5194/cp-10-1165-2014, 2014.
- 705

all journals have been written in full

706